Journal of The Electrochemical Society, **160** (10) C503-C510 (2013)
0013-4651/2013/160(10)/C503/8/$31.00 © The Electrochemical Society

Formation and Crystallization of Anodic Oxide Films on Sputter-Deposited Titanium in Potentiostatic and Potential-Sweep Modes

Jun-Heng Xing, Hui Li, Zheng-Bin Xia,[z] Jian-Feng Hu, Yan-Hong Zhang, and Li Zhong

School of Chemistry and Chemical Engineering, South China University of Technology, Guangzhou, Guangdong 510640, China

Sputter-deposited titanium substrates were anodically treated in sulfuric acid solution both in potentiostatic and potential-sweep modes. The morphology, crystallization, chemical compositions and electrochemical properties of anodic titanium oxide films were detected by AFM, SE, Raman spectra, XPS and EIS. The formed anodic films are smooth and homogeneously crystallized, and that the potentiostatically grown film is slightly thicker and less crystalline than the potentiodynamically formed film. Moreover, a comparison of the structure and properties of the anodic oxides films formed on the mechanical-chemical polished bulk titanium and the sputter-deposited titanium substrates is also presented. The titanium substrates can largely influence the properties of the formed anodic films. A more smooth and compact titanium oxide film could grow on the sputter-deposited titanium substrate, which is unfavorable to the ionic migration through the film and delays the film growth and crystallization.
© 2013 The Electrochemical Society. [DOI: 10.1149/2.066310jes] All rights reserved.

Manuscript submitted July 10, 2013; revised manuscript received August 9, 2013. Published August 22, 2013.

Thin anodic oxide films on titanium are well-known for their high corrosion resistance,[1] good biomedical compatibility[2,3] and excellent photocatalytic activity.[4,5] The crystalline structure, surface morphology, chemical compositions and electrochemical properties of anodic films on titanium are influenced by various anodization parameters.[6–8] In general, the growth and crystallization of anodic titanium oxide films can be promoted by raising the applied voltage,[7,9,10] prolonging the anodizing time,[10–13] enhancing the solution temperature,[7,14] increasing the electrolyte concentration[12,13] or decreasing the film growth rate.[15,16] With the incorporation of impurity ions (anions from the electrolytic solution[17] or cations from the titanium alloy)[18–20] in the anodic titanium oxide layers, the film crystallization is suppressed to relatively high voltages. Besides, as compared to the slow-grown anodic titanium oxide films (in potential-sweep mode or galvanostatic mode), the fast-grown films (in potentiostatic mode) are much thicker and more crystalline.[8,21–23]

The preparation and surface pretreatment of titanium substrates can also influence the formation and crystallizing process of anodic titanium oxide films. Generally speaking, commercial pure titanium sheets or highly pure titanium plates are the most common specimens used for titanium anodization, and the samples are usually pretreated by mechanical polishing and (or) chemical polishing before electrochemical treatments. As compared to the anodic films produced on unpolished titanium substrates, the films grown on mechanical polished titanium surface are smoother and more compact and have a better corrosion resistance.[11] The chemical polishing of titanium substrates prior to anodization also plays an important role in the anodic film formation. For instance, Kozlowski et al. revealed that crystalline titanium oxides could be only obtained after the naturally formed oxide film on the titanium surface (with the thickness of about 5 nm) was removed by chemical etching.[24,25] However, for the titanium samples etched by strong acid solutions (HNO_3 or HF), Prusi et al. proposed that it would dissolve fast during the anodizing process, hence this treatment is unfavorable for the growth of anodic titanium oxide films.[12]

Even for the mechanical-chemical polished titanium samples, their surface still contains numerous local defects. Therefore, others have used deposited titanium thin film samples, prepared by ion-beam sputtering methods, as the working electrode.[26–29] The titanium films deposited on silicon wafer substrates are very smooth, with the average roughness usually smaller than 1 nm, depending on the preparation conditions. There are at least three advantages of using atomically flat sputter-deposited titanium substrates for the preparation of titania anodic films. Firstly, the anodic films grown on deposited titanium samples are much more smooth and compact, which makes them more suitable for use in many application areas, such as corrosion protection[30] and photocatalytic engineering.[31,32] Secondly, with the homogeneous and smooth anodic films grown on deposited titanium, the film growth and crystallization behavior can be studied by characterization techniques that are sensitive to the film uniformity and surface roughness, such as scanning tunneling microscopy (STM, used to detect the atom arrangement of titanium oxides),[26,33,34] spectroscopic ellipsometry (SE, used to determine the film optical properties)[26,35] and in situ curvature measurements (used to estimate the film internal stresses).[28,36] Specific titanium alloys, which can be easily obtained by sputtering deposition methods, can be used for the fabrication of functional materials[37,38] and for some special studies in titanium anodization (such as the ionic transport behavior).[19,39]

Since the sputter-deposited titanium specimens play an important role in the preparation of functional anodic titanium oxide films, it is necessary to study the growth and crystallization behavior of anodic films on deposited titanium in different anodization modes. However, up to now, this subject has been seldom addressed.[21] Moreover, it is obvious that the titanium substrate morphology can largely influence the structure and properties of anodic oxide layers.[11,40,41] Therefore, a comparison of the properties of the formed anodic films between the common mechanical-chemical polished titanium substrates and the smooth sputter-deposited titanium samples will be beneficial to the understanding of titanium anodization.

In previous work,[8] we reported the influence of anodization modes on the structure and properties of anodic films grown on mechanical-chemical polished highly pure titanium substrates, and we also proposed a model about the formation and crystallizing mechanisms of titanium oxide films under different conditions. It was revealed that the local defects of titanium substrates played a key role on the formation of "flower-like" titania crystalline grains in potentiostatic mode. In the present study, the atomically flat sputter-deposited titanium samples are anodically treated in potentiostatic and potential-sweep modes. The influence of film growth modes on the properties of anodic titanium oxide films is studied, the growth and crystallizing mechanisms of anodic oxide films on sputter-deposited titanium in different anodization modes are proposed. Moreover, a comparison of the surface features, crystalline behavior, chemical compositions and electrochemical properties of the formed titanium oxide films between the mechanical-chemical polished titanium samples and the sputter-deposited titanium substrates is presented, and the effect of titanium substrates on the growth and crystallization of anodic titanium oxide films is also discussed.

Experimental

Sample preparation.— Titanium films with a thickness of about 500 nm were deposited onto silicon wafer substrates by the magnetron

[z]E-mail: cezhbxia@scut.edu.cn

Downloaded on 2013-08-27 to IP 210.72.158.175 address. Redistribution subject to ECS license or copyright; see ecsdl.org/site/terms_use

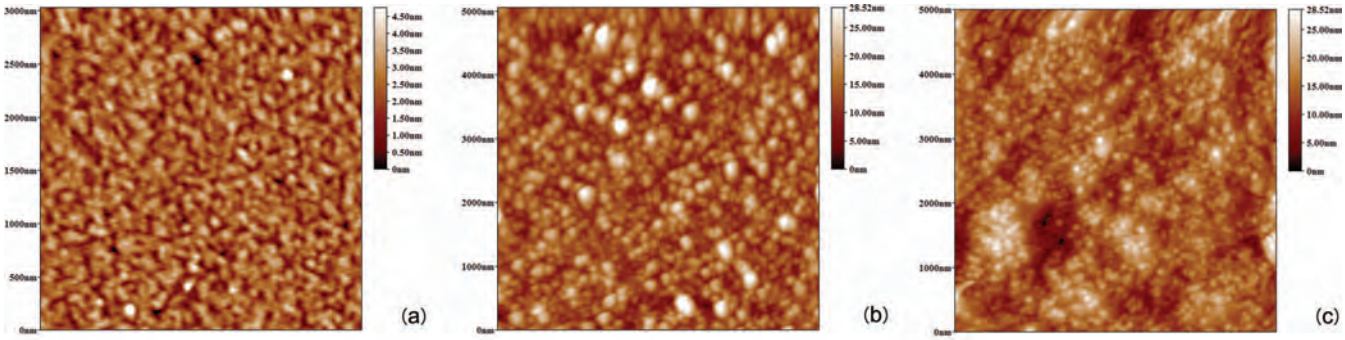

Figure 1. AFM images of (a) sputter-deposited titanium substrate and anodic films on titanium formed in (b) potentiostatic and (c) potential-sweep modes.

sputtering method. The sputter target was a disk-shaped titanium plate (99.99%) with the diameter of 60 mm and the thickness of 3 mm. The deposited specimens were then diced into small sheets of 10 × 10 mm in size and used as a working electrode. Before anodization treatments, the as-deposited titanium substrates were ultrasonically cleaned with acetone for 20 min and later with deionized water for 20 min.

Anodization procedure.— The sputter-deposited titanium samples were electrochemically treated in a two-electrode electrochemical cell. A platinum plate was used as the counter electrode, and 0.1 M H_2SO_4, prepared by analytical reagent and high purity water, was used as the electrolyte. An electrochemical workstation (Metrohm Autolab PGSTAT100, Switzerland) equipped with a Voltage Multiplier module was used to maintain the anodization procedure. The sulfuric acid solution was stirred with purified nitrogen gas before and during the anodic films formation, and all experiments were carried out at a constant temperature of 25°C. The titanium anodization was performed both in potentiostatic and potential-sweep modes. For the potentiostatic mode, the applied voltage of 30 V was used and the anodizing time was set as 60 min. In the case of the potential-sweep mode, the potential was swept from 0 to 30 V with a potential scanning rate of 0.01 V/s. After anodization treatments, the samples were immediately removed from the solution, rinsed with distilled water for several times, dried by air blowing, and then conserved in a vacuum drying oven before further characterization.

Film characterization.— Atomic force microscopy (AFM, Benyuan CSPM 4000, China) was used to determine the surface morphology of anodic films on titanium. SE (HORIBA Jobin Yvon Auto SE, France) was used to detect the thickness and optical properties of anodic titanium oxide films, and a two layer model (Si substrate/sputter-deposited Ti layer/TiO_2 film) was used in the modeling procedure. The Raman spectra and optical microscopy images of the anodized samples were recorded by a LabRAM Aramis (HORIBA Jobin Yvon, France) instrument which was equipped with an Olympus microscope (Japan). X-ray photoelectron spectrometry (XPS, Kratos Axis Ultra DLD, UK) was use to detect the chemical compositions of anodic oxide films. The electrochemical properties of anodic titanium oxide films were measured by electrochemical impedance spectroscopy (EIS) which were performed in 50 g/L NaCl by potentiostatic mode at open-circuit potentials, with single amplitude of 10 mV and the frequency range of 10^{-2} to 10^5 Hz. All of the measurements were performed more than five times on different locations of the anodized titanium specimens, and the results showed good reproducibility (with the error less than 30%). More detailed information about the characterization methods of anodic oxide films on titanium could be seen from our previous works.[8,10]

Results

Surface topography.— Fig. 1 presents the AFM images of the sputter-deposited titanium substrate and the anodic titanium oxide films obtained in potentiostatic and potential-sweep anodization modes. As shown in Fig. 1a, the as-deposited titanium sample is very flat. In contrast, after the anodizing treatment, the samples become rougher and nonuniform due to the formation of titanium oxides. The surface appearance of anodic titanium oxide films formed in different anodization modes has some differences. The surface of the titanium oxide film grown in potentiostatic mode is covered with numerous small grains with the size ranging from 100 nm to 300 nm (Fig. 1b), and as revealed in the literature, these grains could be mainly composed of titania microcrystals.[26,33] In the case of potential-sweep mode, the formed anodic film is also filled with many titania microcrystals. Unlike the potentiostatically grown film, the small grains on potentiodynamically treated sample surface have a homogeneous size of about 100 nm (Fig. 1c). Moreover, the titanium oxide layer formed in potential-sweep mode is more undulating as compared to the potentiostatically grown film (Fig. 1b and 1c). This phenomenon may imply that for the titanium oxide film formed in potential-sweep mode, the titania microcrystals aggregate to form large semispherical clusters. Similar findings have been also reported by Delplancke et al.[42]

Table I summarizes the thickness and surface roughness of the as-deposited titanium substrate and the anodic oxide films grown in different modes. The average roughness (R_a) and the root mean square roughness (R_{ms}) of the samples were obtained from the AFM results, and the thickness of the anodic films was detected by SE. As can be seen, the potentiostatically grown film is slightly thicker than the anodic film produced in potential-sweep mode. In addition, although the AFM images show that the surface features of the titanium oxide films formed in different anodization modes have some differences, their surface roughness is very close to each other. Therefore, it can be concluded from Table I that the thickness and surface roughness are mainly determined by the applied maximum potentials for the anodic oxide films grown on sputter-deposited titanium substrates.

Crystallization.— The Raman spectra and optical microscopy images of titanium samples anodically oxidized in different modes are displayed in Fig. 2. Both the fast-grown film and the slow-grown film are crystalline (Fig. 2a). Similar to the surface features, the crystalline behavior of the anodic films formed under different conditions also has some differences. For the potentiostatically grown film, four Raman bands at about 144 cm^{-1}, 399 cm^{-1}, 516 cm^{-1} and 639 cm^{-1}, corresponding to anatase type of titanium oxides, can be found. Except

Table I. Thickness and surface roughness of sputter-deposited titanium substrate and anodic titanium oxide films formed in potentiostatic and potential-sweep anodization modes.

Anodization modes	*d* (nm)	R_a (nm)	R_{ms} (nm)
Titanium substrate	–	0.54	0.67
Potentiostatic	36.5	3.00	3.84
Potential-sweep	32.5	2.95	3.77

Downloaded on 2013-08-27 to IP 210.72.158.175 address. Redistribution subject to ECS license or copyright; see ecsdl.org/site/terms_use

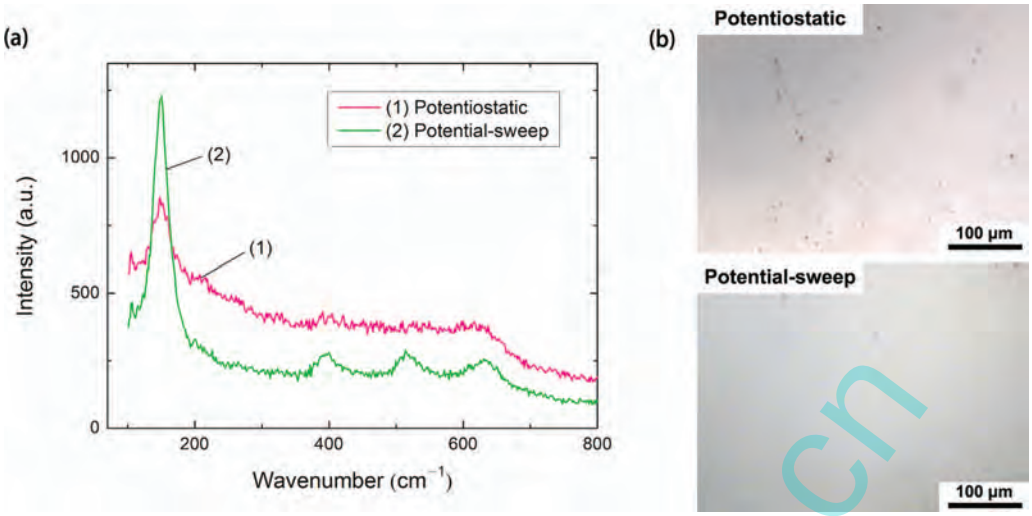

Figure 2. (a) Raman spectra and (b) optical microscopy images of anodic oxide films on sputter-deposited titanium formed in potentiostatic and potential-sweep modes.

for the Raman peak at 144 cm^{-1} (gives indication of the long-range order of anatase phase), the other three Raman peaks (indicate the short-range order of anatase phase) are weak and broad, which may imply that the formed anodic film is weakly crystallized. By contrast, in the case of the potentiodynamically grown film, four Raman bands of anatase can be clearly detected, which means that the anodic film is well crystallized. Moreover, the Raman spectra were taken from different locations of the anodic film surface more than seven times for each anodized specimen, and the results showed good reproducibility within an error limit of about 15% for both the fast-grown film and the slow-grown film. This suggests that the anodic films on sputter-deposited titanium formed in two different anodization modes are both homogeneously crystallized. These findings are in accordance with the optical microscopy pictures, in which both the fast-grown film and the slow-grown film are uniform (Fig. 2b).

It is reported that for very smooth anodic titanium oxide films, the refractive index (n) value is determined by the film structure.[26] For amorphous titania, the n value at the wavelength of 632.8 nm is reported as 2.2, while for anatase titania, n is about 2.55.[43] Table II displays the n value (detected by SE) of anodic oxide films on sputter-deposited titanium formed in different modes. The n value of the formed anodic films is larger than that of the amorphous film but smaller than that of the anatase titanium oxides, indicating that the films are composed of anatase and amorphous titanium oxides. As mentioned by Nanjo et al., if the percentage content of the amorphous oxides is set as x, the crystallinity of the anodic films on sputter-deposited titanium can be calculated from:[26]

$$x = \frac{n_{\text{anatase}} - n_{\text{film}}}{n_{\text{anatase}} - n_{\text{amorphous}}} \quad [1]$$

The crystallinity of anodic oxide films formed in different modes is shown in Table II, from which it is clearly that the crystallinity of the slow-grown film is higher than that of the fast-grown film. It is worth noting that the measured optical constant of titanium oxide films can be also influenced by the film surface roughness (or porosity).[35] Therefore, considering the rough anodic films formed in this work (compared to the smooth films grown at very low voltages),[26] the crystallinity of titanium oxide films shown in Table II should be lower than it actually is.

Table II. Refractive index (at the wavelength of 632.8 nm) and crystallization degree of anodic films on sputter-deposited titanium formed in different modes.

Anodization modes	n	Amorphous (%)	Anatase (%)
Potentiostatic	2.427	35.14	64.86
Potential-sweep	2.479	20.29	79.71

Chemical compositions.— The XPS spectra of anodic films on sputter-deposited titanium obtained under potentiostatic and potential-sweep conditions are displayed in Fig. 3. For the potentiostatically grown film, the Ti 2p spectrum can be resolved into 8 peaks, corresponding to Ti, Ti^{2+}, Ti^{3+} and Ti^{4+}, respectively (Fig. 3a). By contrast, the Ti 2p spectrum of the potentiodynamically grown film can be only disintegrated into 2 peaks, both attributed to Ti^{4+} (Fig. 3b). In contrast to the Ti 2p spectra, the O 1s spectra of the anodic films formed in two different modes can be both fitted with 3 peaks, corresponding to O^{2-}, OH^- and H_2O, respectively (Fig. 3c and 3d). The percentages of each species from the Ti 2p and O 1s spectra of anodic films on sputter-deposited titanium formed by different modes are summarized in Table III. The concentrations of the Ti^{4+} and O^{2-} species are much higher for the film grown in potential-sweep mode. This implies that for the anodic film on sputter-deposited titanium, the slow growth process is beneficial to the conversion of titanium suboxides (TiO and Ti_2O_3) into titania and also promotes the film dehydration. The titanium suboxides and absorbed water (OH^- and H_2O) in the film are both unfavorable for the crystallization of anodic titanium oxides.[26,44]

Table III. Peak position and percentage contents of the surface species from Ti 2p and O 1s spectra of anodic films on sputter-deposited titanium formed in potentiostatic and potential-sweep modes.

Spectrum	Surface species	Peak position (eV)	Peak area (%) Potentiostatic	Peak area (%) Potential-sweep
Ti 2p 3/2	Ti	453.58	3.29	–
	Ti^{2+}	454.72	3.09	–
	Ti^{3+}	456.37	5.03	–
	Ti^{4+}	458.31	61.63	65.89
Ti 2p 1/2	Ti	459.86	0.65	–
	Ti^{2+}	460.38	2.32	–
	Ti^{3+}	462.09	2.75	–
	Ti^{4+}	464.05	21.34	34.11
O 1s	O^{2-}	529.54	59.90	68.20
	OH^-	531.13	24.63	19.63
	H_2O	532.46	15.47	12.17

www.sjm.com.cn

Downloaded on 2013-08-27 to IP 210.72.158.175 address. Redistribution subject to ECS license or copyright; see ecsdl.org/site/terms_use

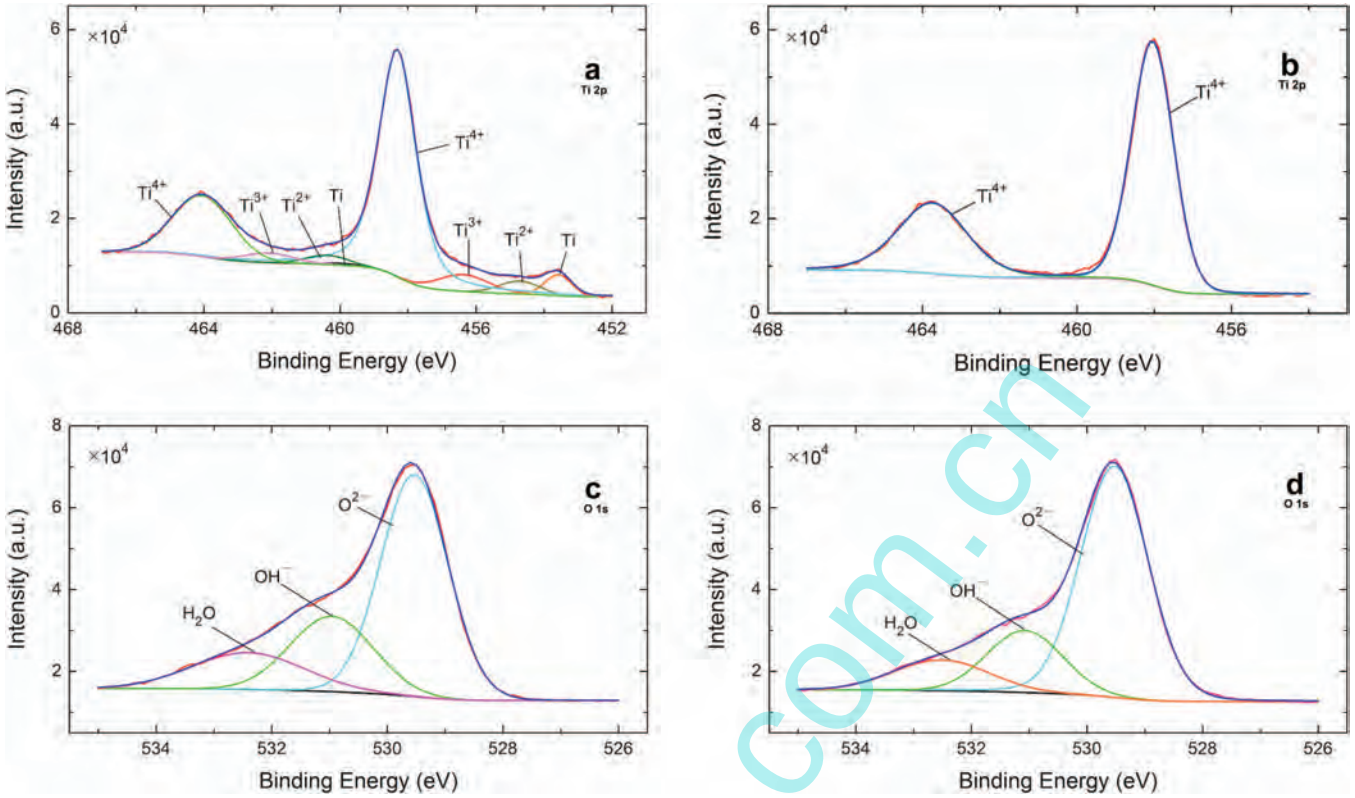

Figure 3. Ti 2p and O 1s XPS spectra of anodic films on sputter-deposited titanium produced in (a, c) potentiostatic and (b, d) potential-sweep modes.

That could be one reason why the crystallinity of the slow-grown film is higher than that of the fast-grown film (see Fig. 2a and Table II).

EIS.— The Bode plot of the electrochemical impedance data of anodic films on sputter-deposited titanium formed by different modes is shown in Fig. 4a and 4b. The equivalent circuit model, which is shown in Fig. 4c, is used to simulate the obtained experimental data, and the fitting curves can also be found in Fig. 4a and 4b. Very good agreement between the fitting curves and the experimental data can be seen, which means that the produced anodic films on sputter-deposited titanium contain two layers: an outer porous layer and an inner barrier layer. Table IV displays the equivalent circuit parameters for anodic oxide films on sputter-deposited titanium formed by different modes. The porous layer resistance (R_{pr}) of the fast-grown film is slightly lower than that of the slow-grown film, which means that the porosity should be a little higher for the potentiostatically grown film. By contrast, the barrier layer resistance (R_b) is slightly higher for the anodic oxide film produced in potentiostatic mode, which is probably because that the crystallinity of the fast-grown film is lower than that of the slow-grown film (see Table II).

The capacitance (C) and thickness of the porous layer and barrier layer of the formed anodic titanium oxide films can be calculated by using the methods presented in previous works,[8,45] and the results are shown in Table V. It is found that the porous layer capacitance (C_{pr}) is lower for the anodic film formed by potentiostatic mode. This fact could be an indication that, compared to the potentiodynamically grown film, the porous layer is thicker and the film crystallinity is lower for the potentiostatically formed film. By contrast, because the film crystallinity is slightly lower and the inner layer is much thinner for the fast-grown film, its barrier layer capacitance (C_b) is a little larger than the slow-grown film. The dielectric constant (ε) of anodic films on titanium was considered to be 48 (i.e. the ε value of anatase) in the previous work,[8] while in the present study, the produced anodic films on sputter-deposited titanium are proved to be composed of anatase and amorphous oxides (especially for the fast-grown film, see Fig. 2 and Table II). Therefore, the actual thickness of the barrier layer of the anodic films should be a little thinner than the values presented in Table V.

Table V. Outer and inner layer capacitance and barrier layer thickness for titanium oxide films anodically grown in different modes.

Anodization modes	C_{pr} (μF/cm^2)	C_b (μF/cm^2)	d of inner layer (nm)
Potentiostatic	21.72	3.371	12.6
Potential-sweep	36.01	2.822	15.05

Discussion

Growth and crystallization of anodic films on sputter-deposited Ti.— The evolution of current density with anodizing time (or potential) for anodization of sputter-deposited titanium in different modes is presented in Fig. 5. The current evolution of films growth on sputter-deposited samples is similar to that of high purity titanium

Table IV. Equivalent circuit parameters for anodic films on sputter-deposited titanium formed in different anodization modes.

Anodization modes	R_s (Ω)	R_{pr} (kΩcm^2)	Q_{pr} (s^n/Ωcm^2)	n_1	R_b(kΩcm^2)	Q_b (s^n/Ωcm^2)	n_2
Potentiostatic	16.05	18.3	1.645×10^{-5}	0.9049	126.2	2.958×10^{-6}	0.9553
Potential-sweep	12.4	29.1	2.682×10^{-5}	0.9125	108.1	2.506×10^{-6}	0.9647

Downloaded on 2013-08-27 to IP 210.72.158.175 address. Redistribution subject to ECS license or copyright; see ecsdl.org/site/terms_use

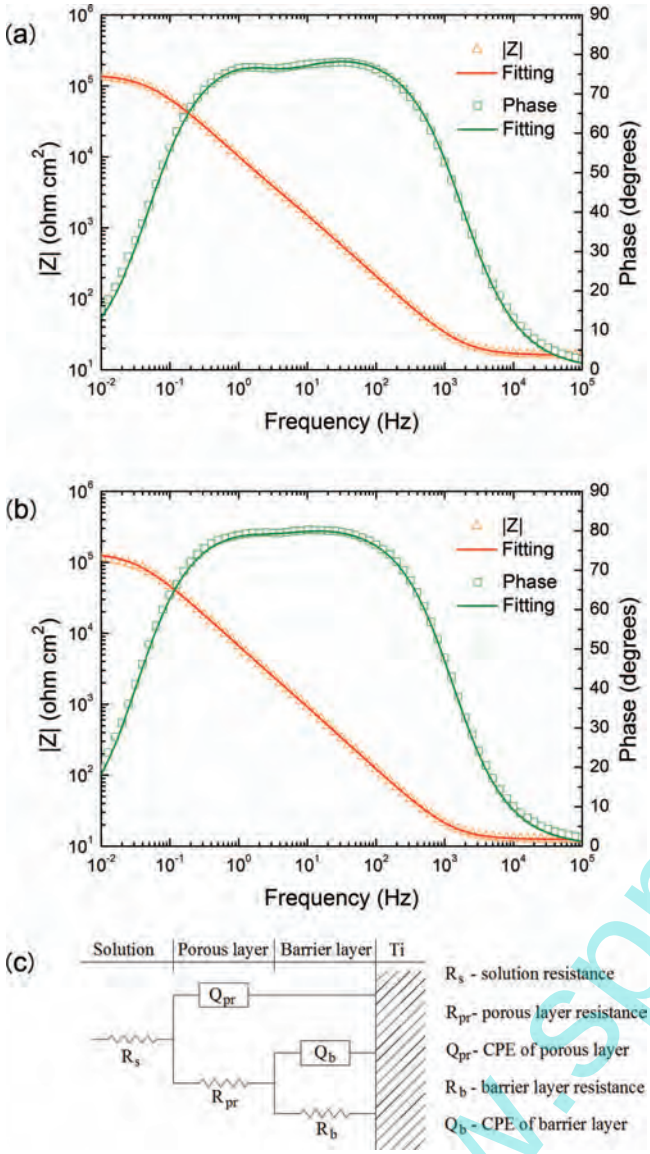

Figure 4. Bode diagram of impedance data and fitting curves of anodic films on sputter-deposited titanium formed under (a) potentiostatic and (b) potential-sweep conditions, and (c) equivalent circuit model used for simulating EIS results.

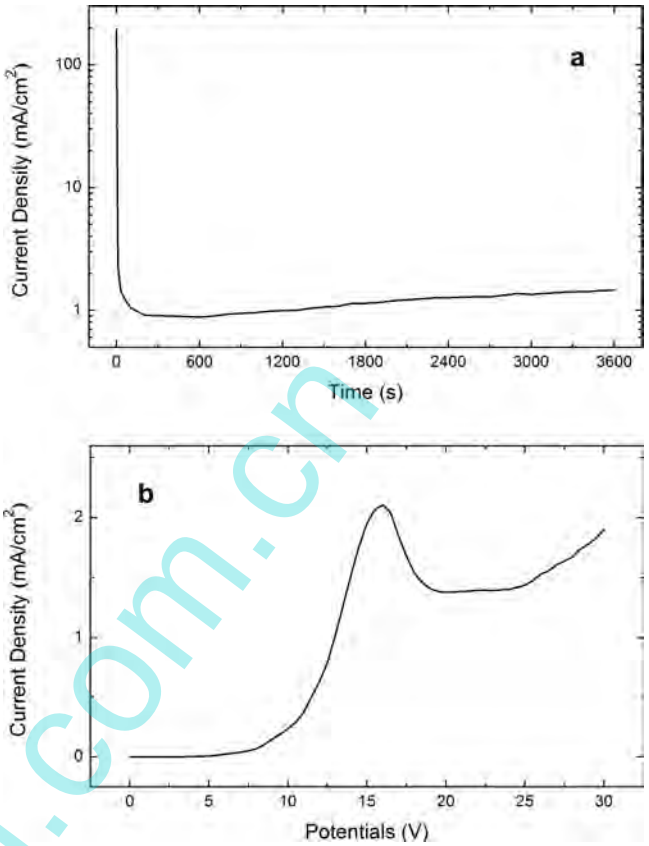

Figure 5. Evolution of current density with anodizing time (or oxidation potentials) for anodic films formed on sputter-deposited titanium in (a) potentiosatic and (b) potential-sweep modes.

anodization.[8] Under potentiostatic condition, the current density is very large at the very beginning stage of anodizing process. As a result, a layer of titanium oxide quickly forms in milliseconds, and meanwhile TiO_2 nanocrystals with various sizes randomly emerge. With increasing time, these nanocrystals grow up to microcrystals and distribute throughout the film surface (see Fig. 1b). Because the formation of these microcrystals is independent of each other, the bulk film is not well crystallized (see Fig. 2a).

For titanium anodization in potential-sweep mode, the current density starts at about zero and increases with potential. The growth and crystallization of anodic films is a relatively slow process. The titania microcrystals homogeneously emerge, and some of them are more likely to aggregate to form large semispherical crystalline clusters (see Fig. 1c), making the formed film more crystallized than the fast-grown film (see Fig. 2a). It is worth noting that a peak current can be seen at about 16 V, and this is a result of the oxygen evolution reaction (OER).[17] Moreover, as revealed by XPS, the slow growth process is beneficial to the film dehydration (see Table III). In other words, the slow-grown film is more compact,[23] and this could be the main reason why the anodic film formed in potential-sweep mode is slightly thinner than the potentiostatically grown film.

Comparison of film properties for two different Ti substrates.— As stated above, we present the structure and properties of anodic films on sputter-deposited titanium formed in potentiostatic and potential-sweep modes, and the properties of the oxide films grown on mechanical-chemical polished highly pure titanium bulk substrates by different anodization modes can be found in our previous study.[8] Therefore, a comparison of the structure, morphology and composition of the formed anodic films is made between the two different titanium substrates.

As revealed by Raman spectroscopy and SE measurements, whatever anodization mode is performed, the anodic films grown on polished bulk titanium are all thicker and more crystalline than the ones grown on sputter-deposited titanium substrates.

For the mechanical-chemical polished titanium specimens, the crystallization behavior is different for the films formed in different anodization modes: the potentiostatically grown film is heterogeneously crystallized, while crystallization of the potentiodynamically formed film is homogeneous. For the sputter-deposited titanium samples, the formed anodic films in two different modes are both homogeneously crystallized. Moreover, the fast-grown film is more crystalline than the slow-grown film for the highly pure titanium samples, while in the case of sputter-deposited titanium specimens, the crystallinity is higher for the anodic film formed in potential-sweep mode.

The anodization mode has a great influence on the growth of the anodic films on mechanical-chemical polished titanium; the fast-grown film is much thicker than the slow-grown film. By contrast, for the sputter-deposited titanium samples, the anodic films thickness is mainly determined by the maximum voltage; the potentiostatically grown film is only slightly thicker than the film produced by the

Downloaded on 2013-08-27 to IP 210.72.158.175 address. Redistribution subject to ECS license or copyright; see ecsdl.org/site/terms_use

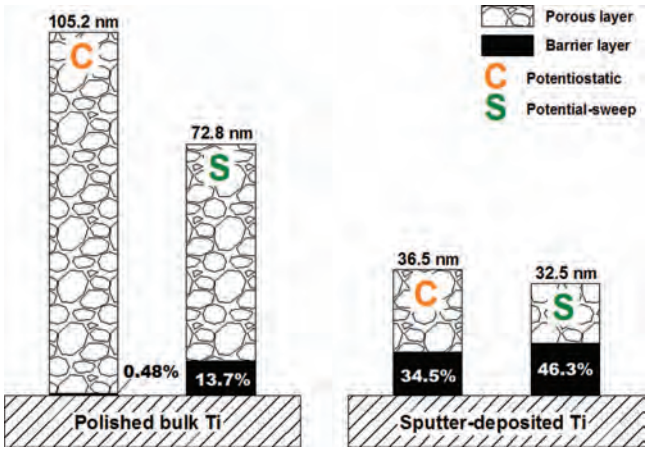

Figure 6. Comparison of porous layer and barrier layer thickness for anodic films produced on different titanium substrates by potentiostatic and potential-sweep modes.

potential-sweep mode. Moreover, as can be seen from Fig. 6, under a given anodization condition, the percentage thickness of the barrier layer, obtained from the ratio of the barrier layer thickness to the total film thickness, is much higher for the anodic film grown on sputter-deposited titanium. In addition, for the oxide films grown on the same titanium substrate, the percentage thickness of the barrier layer of the slow-grown film is much higher than that of the fast-grown film.

In the case of the polished bulk titanium substrates, the surface topography of the formed oxide films is influenced by the film preparation modes; many randomly distributed "flower-like" grains can be seen on the potentiostatically grown film, while the film produced in potential-sweep mode is smoother and more compact. For the sputter-deposited titanium samples, although the morphology of the anodic films formed in different modes shows some differences, their surface roughness is very close to each other.

The anodic films grown on highly pure titanium substrates are mainly composed of TiO_2, while for the film potentiostatically grown on sputter-deposited titanium, a small amount of Ti, Ti^{2+} and Ti^{3+} species can be also detected. Similarly, the oxide films formed on mechanical-chemical polished titanium substrates contain larger contents of O^{2-} species as compared to the anodic films grown on sputter-deposited titanium with the same preparation conditions.

The resistance values (R_{pr} or R_b) of the anodic films on sputter-deposited titanium are higher than that of the films grown on highly pure titanium. The C_{pr} of the anodic film potentiostatically formed on mechanically-chemically polished titanium is much larger than the other three films.

Influence of Ti substrates on growth and crystallization of Ti oxide films.— The main difference between the mechanical-chemical polished high purity titanium samples and the sputter-deposited titanium samples is the surface appearance. The latter (with the R_{ms} of 0.67 nm, see Table I) are much smoother than the former (with the R_{ms} of 37.0 nm).[8] As a result, the anodic films grown on sputter-deposited titanium substrates are much more uniform and compact and have a thicker barrier layer (see Fig. 6), which is unfavorable to the ionic migration through the films during titanium anodization. This is in agreement with the anodization curves: for anodic films grown on two different titanium substrates (in potentiostatic mode or in potential-sweep mode), the final current density is much higher for the anodizing of polished bulk titanium samples (see Fig. 5 and Ref. 8). In addition, for titanium anodization under potential-sweep condition, the peak current emerges at about 10 V for highly pure titanium[8] and at about 16 V for sputter-deposited titanium samples (see Fig. 5b), indicating that the OER is delayed for the anodic films grown on smooth titanium substrates.

The ionic migration plays a key role on the growth and crystallization of anodic titanium oxide films.[17] As reported by Habazaki et al., the titanium oxides are formed at the oxide/solution interface by the migration of titanium ions outward and at the metal/oxide interface by the migration of anions (O^{2-} and OH^-) inward, and the cationic transport number is about 0.38.[19,39] In addition, the crystallization of anodic films on titanium is mainly promoted by local heating (i.e. the local current density) and mechanical energy (i.e. the internal compressive stresses), which are both influenced by the ionic transport through the films.[8,16,46,47] In other words, the film growth and crystallization can be promoted by enhancing the ionic conductivity of anodic films. Based on the above discussion, the differences of film properties between two different titanium substrates which are presented above can be explained.

As mentioned above, the smooth and compact layers formed on deposited titanium are unfavorable to the ionic transport during titanium anodization. This could be the main reason why the anodic films grown on sputter-deposited titanium substrates are thinner and less crystallized as compared to the films formed on mechanical-chemical polished titanium.

A comparison of the growth and crystallization of potentiostatically formed anodic films between two different titanium samples is shown in Fig. 7. For the anodization of the polished bulk titanium substrates in potentiostatic mode, the titania microcrystals initially emerge at the local defect sites due to very high local current density. With increasing anodizing time, these microcrystals act as ionic conduction channels and grow to "flower-like" TiO_2 crystalline grains. By contrast, for the anodic films grown on sputter-deposited titanium in potentiostatic mode, there is no high local current density for the reason that the samples are very smooth (i.e. have no apparent defects, see Fig. 1a). Instead, titania nanocrystals are randomly formed due to the large current density in the beginning stage of anodizing process (see Fig. 5a). Furthermore, because of the formed compact titanium oxide layers, these nanocrystals do not act as ionic conduction channel, and hence will not grow to large titania crystalline grains. In contrast to the anodic film potentiostatically grown on mechanical-chemical polished titanium, the crystallization of the fast-grown film on deposited titanium is mainly induced by the compressive stresses. However, for titanium anodization in potentiodynamic mode, the differences between two different titanium substrates are not so evident. Because the growth and crystallization of anodic films go through a very slow process, the films grown on two different titanium substrates are both homogeneously crystallized. Moreover, as presented above, the crystalline clusters are generated for anodic films produced on sputter-deposited titanium in potential-sweep mode. This is why the slow-grown film is more crystalline than the fast-grown film. By contrast, for the polished bulk titanium specimens, due to the formation of large titania crystalline grains, the potentiostatically formed film is more crystalline than the film grown in potential-sweep mode.

For the polished bulk titanium samples, the large crystalline grains formed in potentiostatic mode (and perhaps the porous region between the large grains) can act as excellent electronic and ionic conduction channels, and then promote the growth of titanium oxide films. Therefore, the fast-grown film is much thicker than the slow-grown film. By contrast, in the case of sputter-deposited samples, although similar TiO_2 nanocrystals emerge at the beginning stage of the potentiostatic anodization process, these nanocrystals cannot act as good ionic conduction channels due to the formed smooth and compact anodic film (see Fig. 7). As a result, the film growth is less affected by the anodization mode. Moreover, the surface features of titanium substrates can influence the structure of the formed anodic films. As compared to the mechanical-chemical polished titanium substrates, the deposited titanium samples are much smoother, hence the formed anodic films are more compact (i.e. have a much higher percentage thickness of the barrier layer). Similarly, the anodization mode can also affect the structure of the formed films; the slow-grown film is much more compact than the fast-grown film.

In the case of highly pure titanium samples, "flower-like" crystalline grains are produced due to very high local current density at

Downloaded on 2013-08-27 to IP 210.72.158.175 address. Redistribution subject to ECS license or copyright; see ecsdl.org/site/terms_use

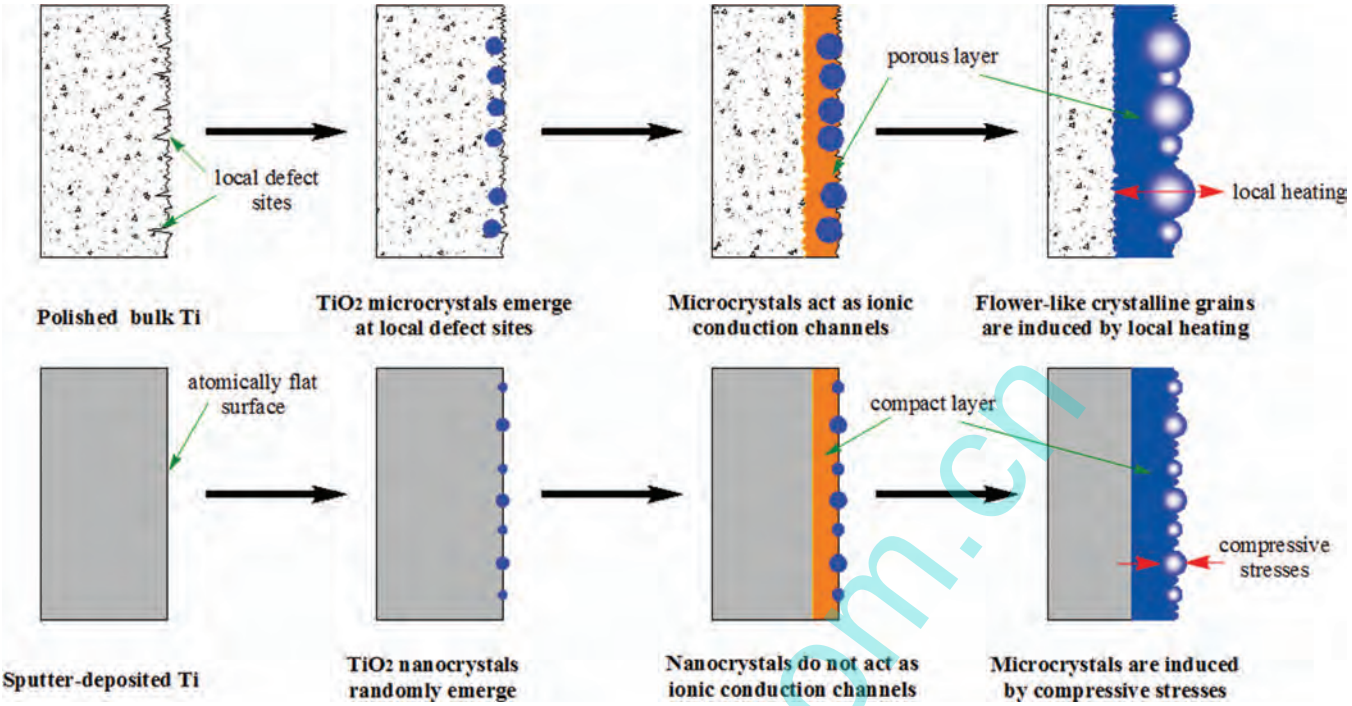

Figure 7. Schematic illustration of formation and crystallizing mechanisms of anodic oxide films on mechanical-chemical polished titanium and sputter-deposited titanium substrates under potentiostatic condition.

the defect sites. The very smooth deposited titanium samples have no apparent local defects, hence cannot form large titania crystalline grains.

It has been reported that the initially formed anodic oxides on titanium are mainly composed of TiO_2, and also contain a number of titanium suboxides and hydrated titanium oxides.[26,48] Generally speaking, high oxidation voltages are beneficial to the conversion of titanium suboxides and hydrated titanium oxides into TiO_2. For example, for the final voltage of 30 V, the anodic films grown on high purity titanium samples largely consist of TiO_2.[8] By contrast, in the case of smooth sputter-deposited titanium samples, the conversion of titanium suboxides and hydrate TiO_2 into TiO_2 is affected by the formed compact anodic layer (because the ionic migration is resisted by the compact anodic film). This is why the species of Ti^{2+} and Ti^{3+} and the larger percentage content of OH^- and H_2O are detected for the anodic films grown on deposited titanium substrates (especially for the fast-grown film). As to the small amount of metallic titanium found in the potentiostatically grown film, a possible explanation could be that the sputter-deposited titanium has less local uniformity or stability than the bulk samples. Also, in the very beginning stage of potentiostatic anodization, the chemical reaction is very strong due to very high local current density. As a result, at the metal surface, some metallic titanium may peel off and be incorporated in the oxide film.

As compared to the anodic films produced on mechanical-chemical polished titanium substrates, the films grown on sputter-deposited titanium are much more compact and have a thicker barrier layer (see Figs. 1 and 6). Therefore it is not difficult to imagine that their resistance values (R_{pr} or R_b) are much higher because the film resistance is proportional to the film thickness and inversely proportional to the film porosity. Similarly, the C_{pr} value of the potentiostatically grown film on high purity titanium is much higher because the porous layer of this film is much thicker than the other three (see Fig. 6).

Conclusions

Anodization of sputter-deposited titanium samples was performed in 0.1 M H_2SO_4 solution both in potentiostatic and potential-sweep modes with the final voltage of 30 V. The anodic films grown on sputter-deposited titanium substrates are smooth, compact and homogeneously crystallized. The slow-grown film is slightly thinner and more crystalline than the fast-grown film, and as revealed by XPS, the slow-grown process promotes film dehydration. The EIS results show that the grown anodic films contain an outer porous layer and an inner barrier layer, and the barrier layer of the anodic film formed by potential-sweep mode is thicker than that of the film produced in potentiostatic mode.

The titanium substrates also have a great influence on the properties of the formed anodic films. Because the compact barrier layer grown on smooth sputter-deposited titanium is unfavorable to the ionic transport across the oxide films, the film growth and crystallization process is much different for the deposited samples as compared to the mechanical-chemical polished titanium samples, especially under potentiostatic conditions. As a result, the anodic films grown on sputter-deposited titanium are much thinner and less crystalline than the films formed on highly pure titanium substrates.

Acknowledgments

The authors acknowledge the financial support from the National Natural Science Foundation of China (NSFC, No. 20976058).

References

1. K. Indira, U. K. Mudali, and N. Rajendran, *Ceram. Int.*, **39**, 959 (2013).
2. C. Bayram, M. Demirbilek, N. Caliskan, M. E. Demirbilek, and E. B. Denkbas, *Journal of Biomedical Nanotechnology*, **8**, 482 (2012).
3. W. Simka, A. Sadkowski, M. Warczak, A. Iwaniak, G. Dercz, J. Michalska, and A. Maciej, *Electrochim. Acta*, **56**, 8962 (2011).
4. W. Y. Wang and B. R. Chen, *International Journal of Photoenergy*, **2013**, 348171 (2013).
5. M. N. Liu, J. Chang, H. X. Wang, C. Yan, and J. Bell, *J. Nanosci. Nanotechnol.*, **13**, 1141 (2013).
6. M. V. Diamanti and M. P. Pedeferri, *Corros. Sci.*, **49**, 939 (2007).
7. T. Shibata and Y. Zhu, *Corros. Sci.*, **37**, 253 (1995).
8. J. Xing, Z. Xia, J. Hu, Y. Zhang, and L. Zhong, *J. Electrochem. Soc.*, **160**, C239 (2013).
9. A. G. Mantzila and M. I. Prodromidis, *Electrochim. Acta*, **51**, 3537 (2006).
10. J. Xing, Z. Xia, J. Hu, Y. Zhang, and L. Zhong, *Corros. Sci.*, **75**, 212 (2013).

Downloaded on 2013-08-27 to IP 210.72.158.175 address. Redistribution subject to ECS license or copyright; see ecsdl.org/site/terms_use

11. D. Capek, M. Gigandet, M. Masmoudi, M. Wery, and O. Banakh, *Surf. Coat. Technol.*, **202**, 1379 (2008).
12. A. Prusi, L. Arsov, B. Haran, and B. Popov, *J. Electrochem. Soc.*, **149**, B491 (2002).
13. L. Arsov, C. Kormann, and W. Plieth, *J. Electrochem. Soc.*, **138**, 2964 (1991).
14. T. Shibata and Y. Zhu, *Corros. Sci.*, **37**, 133 (1995).
15. Y. Huang and D. Blackwood, *Electrochim. Acta*, **51**, 1099 (2005).
16. J. Leach and B. Pearson, *Corros. Sci.*, **28**, 43 (1988).
17. H. Habazaki, M. Uozumi, H. Konno, K. Shimizu, P. Skeldon, and G. Thompson, *Corros. Sci.*, **45**, 2063 (2003).
18. H. Habazaki, M. Uozumi, H. Konno, S. Nagata, and K. Shimizu, *Surf. Coat. Technol.*, **169–170**, 151 (2003).
19. H. Habazaki, K. Shimizu, S. Nagata, P. Skeldon, G. Thompson, and G. Wood, *Corros. Sci.*, **44**, 1047 (2002).
20. H. Habazaki, M. Uozumi, H. Konno, K. Shimizu, S. Nagata, K. Asami, K. Matsumoto, K. Takayama, Y. Oda, and P. Skeldon, *Electrochim. Acta*, **48**, 3257 (2003).
21. P. Bourdet, F. Vacandio, L. Argeme, S. Rossi, and Y. Massiani, *Thin Solid Films*, **483**, 205 (2005).
22. S. Kudelka, A. Michaelis, and J. Schultze, *Electrochim. Acta*, **41**, 863 (1996).
23. D. Wiesler and C. Majkrzak, *Physica B: Condensed Matter*, **198**, 181 (1994).
24. M. R. Kozlowski, P. S. Tyler, W. H. Smyrl, and R. T. Atanasoski, *Surf. Sci.*, **194**, 505 (1988).
25. M. Kozlowski, W. H. Smyrl, L. Atanasoska, and R. Atanasoski, *Electrochim. Acta*, **34**, 1763 (1989).
26. Z. Xia, H. Nanjo, H. Tetsuka, T. Ebina, M. Izumisawa, M. Fujimura, and J. Onagawa, *Electrochem. Commun.*, **9**, 850 (2007).
27. Q. Van Overmeere, J. Vanhumbeeck, and J. Proost, *J. Electrochem. Soc.*, **157**, C166 (2010).
28. J. Vanhumbeeck and J. Proost, *J. Electrochem. Soc.*, **155**, C506 (2008).
29. J. Vanhumbeeck, L. Ryelandt, and J. Proost, *Electrochim. Acta*, **54**, 3330 (2009).
30. E. Akiyama, H. Yoshioka, J. Kim, H. Habazaki, A. Kawashima, K. Asami, and K. Hashimoto, *Corros. Sci.*, **34**, 27 (1993).
31. S. Z. Chu, S. Inoue, K. Wada, S. Hishita, and K. Kurashima, *Adv. Funct. Mater.*, **15**, 1343 (2005).
32. A. Kar, R. Pando, and V. Subramanian, *J. Mater. Res.*, **25**, 82 (2010).
33. Z. Xia, H. Nanjo, T. Aizawa, M. Kanakubo, M. Fujimura, and J. Onagawa, *Surf. Sci.*, **601**, 5133 (2007).
34. H. Nanjo, M. Fujimura, N. Laycock, Z. Xia, M. Nishioka, I. Ishikawa, and J. Onagawa, *Current Applied Physics*, **6**, 448 (2006).
35. H. Nanjo, Y. Yao, Z. Xia, M. Nishioka, Y. Hiejima, and M. Kanakubo, *e-Journal of Surface Science and Nanotechnology*, **3**, 345 (2005).
36. J. F. Vanhumbeeck, H. Tian, D. Schryvers, and J. Proost, *Corros. Sci.*, **53**, 1269 (2011).
37. T. Lindgren, J. M. Mwabora, E. Avendaño, J. Jonsson, A. Hoel, C. G. Granqvist, and S. E. Lindquist, *The Journal of Physical Chemistry B*, **107**, 5709 (2003).
38. V. Nettikaden, A. Baron-Wiecheć, P. Bailey, T. Noakes, P. Skeldon, and G. Thompson, *Corros. Sci.*, **52**, 3717 (2010).
39. H. Habazaki, K. Shimizu, S. Nagata, P. Skeldon, G. E. Thompson, and G. C. Wood, *J. Electrochem. Soc.*, **149**, B70 (2002).
40. M. Dubey and H. He, *Nanoscience and Nanotechnology Letters*, **4**, 548 (2012).
41. Y. Shin and S. Lee, *Nano Lett.*, **8**, 3171 (2008).
42. J. L. Delplancke, A. Garnier, Y. Massiani, and R. Winand, *Electrochim. Acta*, **39**, 1281 (1994).
43. A. Michaelis, J. Delplancke, and J. Schultze, *Mater. Sci. Forum*, **185–188**, 471 (1995).
44. T. Ohtsuka and N. Nomura, *Corros. Sci.*, **39**, 1253 (1997).
45. C. H. Hsu and F. Mansfeld, *Corrosion*, **57**, 747 (2001).
46. J. Yahalom and J. Zahavi, *Electrochim. Acta*, **15**, 1429 (1970).
47. J. Nelson and R. Oriani, *Corros. Sci.*, **34**, 307 (1993).
48. T. Ohtsuka and T. Otsuki, *Corros. Sci.*, **45**, 1793 (2003).

www.spm.com.cn

Downloaded on 2013-08-27 to IP **210.72.158.175** address. Redistribution subject to ECS license or copyright; see **ecsdl.org/site/terms_use**